

# Thermoelastic Analysis of Sigmoid-Orthotropic FG Plates using Airy Stress Function

F. Farhatnia, *Member, IAENG*, A.H. Malek-Ahmadi

**Abstract**— In this paper, static analysis of functionally graded rectangular plates with orthotropic behavior, subjected to mechanical, thermal and thermo-mechanical loading is presented on the basis of classical plate theory (CPT). The boundary condition is supposed to be four simply supported edges. The mechanical and physical properties are varied in direction of thickness, while the Poisson ratios remain constant. The governing equilibrium equation and compatibility equation with plane stress assumption are solved consequently to consider the displacement. The influences of orthotropic ratio, the intensity of transverse loading and thermal gradient, Young modulus ratio of top and bottom faces of the plate and aspect ratio are studied on bending behavior of plate. In this paper, two samples of FG plate are considered; one is the plate which the lower surface is Alumina( $Al_2O_3$ ) and the mechanical properties of upper surface is the multiplier of the Alumina; the other is the ceramic-metal FG plate(Nickel-Alumina) with orthotropic characteristics of ceramics. The results indicate that by increasing Young modulus ratio, the plate exhibits more resistance against deformation, the neutral plane moves toward the stronger surface and the deflection decreases. If Young modulus ratio increased, the deflection gets lower. In addition, by exposing the plate to greater positive thermal gradient, the sign of stress field is reversed from tensile to compressive distribution.

**Keyword:** bending analysis, functionally graded material, Orthotropic plate, sigmoid FG function, Airy stress function.

## I. INTRODUCTION

NOWADAYS, during development in aerospace technology, the requirement for the production of modern materials, which can withstand severe environmental phenomena including high thermal gradient, is perceived. Therefore, the idea of making gradual changes in composition of new composites, from heat-resistant ceramics and metals with high machinery ability is formed. Particularly, in an environment with high temperature, the thermal expansion coefficient of layers of laminar composites mismatches the severe residual stresses applied to the layers, leading to failure delamination of the layers. Thus the concept of functionally graded materials to eliminate residual stresses due to gradual changes in a desired direction was introduced [1]-[2]. Studies reveal that the application of functionally

graded materials in structures can reduce the residual stress significantly. Two familiar FG models, namely, power law and exponential function are used to describe the mixture variation of the volumetric ratio of metal and ceramics, however in both functions, the stress concentration is observed due to rapid change in the continuity of constituent materials in FGMs. Chi and Chung used the sigmoid function, which is composed of two power-law functions, to model FG behavior in order to define a volume fraction that can reduce the stress intensity factors significantly [3].

Due to functionally graded materials use in aerospace, nuclear, medical industries, several researches have been conducted in the field of dynamic and statics analysis. Herein, we introduced those are related to the present subject. Chi and Chung [4]-[5] investigated the static response of FG rectangular plate based on classical plate theory (CPT) when subjected to transverse loading via analytical method (Airy stress function) and finite element method (FEM). They supposed the mechanical properties vary continuously throughout the thickness direction according to the volume fraction of constituents defined by power-law, sigmoid, or exponential function.

Due to the fact of inherent anisotropy of this kind of materials, study on this characteristics of functionally graded materials when exposed to severe variation in working environment must be noticed [6]-[9]. Morimoto and Tanigawa [10] proposed a linear buckling analysis for orthotropic inhomogeneous rectangular plates for simply supported edge condition under uniform in-plane compression with assuming Young's modulus and shear modulus of elasticity which are continuously changed in the thickness direction according to the power law. Ghanndapour and Alinia[11], Alinia and Ghannadpour[12] proposed the large deflection analysis of rectangular functionally graded plates under pressure load. They obtained the numerical results to study the effects of material properties on the deflection and the stress field through the thickness. Chung and Chen [13] obtained the closed-form solution of functionally graded rectangular plates with two opposite edges simply supported and the other two edges free subjected to a uniform load. The closed-form solution to the problems of FGM plates subjected to transverse loads with two opposite edges simply supported and the other two edges free is not found in the literature. They assumed the material properties of the FGM plates to change continuously throughout the thickness of the plate, according to power-law and sigmoid functions. Zenkour and Alghamdi [14] studied the thermoelastic bending analysis of functionally graded ceramic-metal sandwich. They assumed the mechanical and physical properties to vary according to a power law distribution in terms of the volume fractions of the constituents. Beom[15] proposed the linear anisotropic

Manuscript received January 6, 2017; revised February 6, 2017. This work was supported by Islamic Azad University, Khomeinishahr Branch.

Dr. Fatemeh Farhatnia is an assistant professor in Mechanical Engineering department of Islamic Azad University, Khomeinishahr Branch, Manzaraye Boulevard, Khomeinishahr, Isfahan, Iran.(phone:+98-31,33660011; e-mail: farhatnia@iaukhsh.ac.ir).

Amir-Hossein Malek-Ahmadi was graduated from department of Mechanical Engineering, Khomeinishahr Branch, Islamic Azad University, Khomeinishahr, Isfahan, Iran, (e-mail: malek70fh@yahoo.com).

thermoelastic in-plane problems when the solid is exposed to thermal loading and considered the influence of orthotropy parameter on the thermoelastic stress field. Hourai et al. [16] examined a new higher order shear and normal deformation theory to simulate the thermoelastic bending of FG sandwich plates and investigated the effect of the geometrical parameter of plate and new theory characteristics on plate bending response.

In the present paper, the thermoelastic analysis of FG plate having orthotropic characteristics is considered by Airy stress function. For this purpose, the different sections of the present paper are organized as follows: In Section two, constitutive equations based on orthotropic nonhomogeneous characteristics are presented. In Section three, mathematical expressions for stress resultants and stress couples are rewritten by exploiting Airy stress function and governing equilibrium equations and compatibility equations are expressed in terms of displacement and Airy function. In Section four, the governing equations are solved and in Section five, the numerical results are validated against known data in the literature. This is the first attempt to use Airy stress function to solve thermomechanical problem of FG orthotropic rectangular plates.

## II. CONSTITUTIVE RELATIONS OF FG MATERIALS WITH SIGMOID FUNCTION

Fig. 1 shows a rectangular FG plate of length  $a$ , width  $b$  and thickness  $h$  and the mechanical properties varies across the thickness. A coordinate system is established in which  $(x, y, z)$  the plane is in the middle of surface. Owing to small variation of Poisson ratio across the thickness, it is assumed to be a constant value [4]:

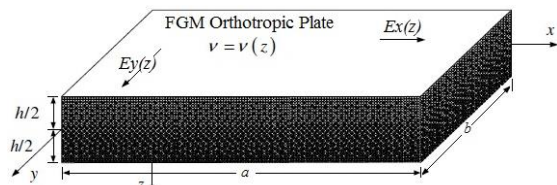


Fig. 1. Schematic of FG plate

$$g_1(z) = 1 - \frac{1}{2} \left( \frac{h/2 - z}{h/2} \right)^p \quad \text{for } 0 \leq z \leq h/2 \quad (1)$$

$$g_1(z) = \frac{1}{2} \left( \frac{h/2 + z}{h/2} \right)^p \quad \text{for } -h/2 \leq z \leq 0$$

$$P(z) = g_1(z)P_1 + (1 - g_1(z))P_2 \quad \text{for } 0 \leq z \leq h/2 \quad (2)$$

$$P(z) = g_2(z)P_1 + (1 - g_2(z))P_2 \quad \text{for } -h/2 \leq z \leq 0$$

$P(z)$  can be represented for Young modulus or thermal expansion coefficient. By applying the Sigmoid power-law function in (1) and (2),  $P_2$  and  $P_1$  is representative for material properties at  $z=-h/2$  and  $z=h/2$ , upper surface and lower one, respectively. The values of Young modulus in the middle plane is the average of Young modulus in two surfaces.

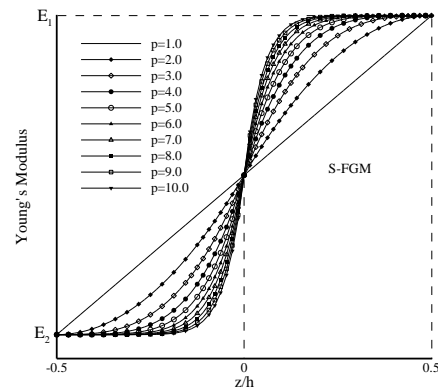


Fig. 2. Variation of Young module in sigmoid model with respect to FG power index

The stress-strain relation in plane-stress conditions with assumption of the plate is exposed to thermal gradient, which is expressed as follows [17]:

$$\begin{bmatrix} \varepsilon_x \\ \varepsilon_y \\ \gamma_{xy} \end{bmatrix} = \begin{bmatrix} 1/E_x(z) & -\nu_{yx}(z)/E_y(z) & 0 \\ -\nu_{xy}(z)/E_x(z) & 1/E_y(z) & 0 \\ 0 & 0 & 1/G_{xy} \end{bmatrix} \begin{bmatrix} \sigma_x \\ \sigma_y \\ \tau_{xy} \end{bmatrix} + \begin{bmatrix} \alpha_x(z)\Delta T \\ \alpha_y(z)\Delta T \\ 0 \end{bmatrix} \quad (3)$$

In addition, the displacement field in any arbitrary point  $(x, y, z)$  of plate may be written as [18]:

$$\begin{cases} u(x, y, z) = u_0(x, y) - z \frac{\partial w}{\partial x} \\ v(x, y, z) = v_0(x, y) - z \frac{\partial w}{\partial y} \\ w(x, y, z) = w_0(x, y) \end{cases} \quad (4)$$

Where  $u_0, v_0, w_0$  denotes displacements of middle surface.

By the assumption of small displacement, the corresponding strain components associated with displacement field (5) are determined as follows:

$$\begin{cases} \varepsilon_x = \frac{\partial u}{\partial x} = \varepsilon_{x_0} - z \frac{\partial^2 w}{\partial x^2} \\ \varepsilon_y = \frac{\partial v}{\partial y} = \varepsilon_{y_0} - z \frac{\partial^2 w}{\partial y^2} \\ \gamma_{xy} = \frac{\partial u}{\partial y} + \frac{\partial v}{\partial x} = \gamma_{xy_0} - 2z \frac{\partial^2 w}{\partial x \partial y} \\ \varepsilon_z = \gamma_{xz} = \gamma_{yz} = 0 \end{cases} \quad (5)$$

From (3) and (5), stress field is presented in terms of strain components in the middle surface and curvatures (6), as follows:

$$\begin{Bmatrix} \sigma_x \\ \sigma_y \\ \tau_{xy} \end{Bmatrix} = \begin{bmatrix} \frac{E_x}{1 - \nu_{xy}\nu_{yx}} & \frac{\nu_{yx}E_x}{1 - \nu_{xy}\nu_{yx}} & 0 \\ \frac{\nu_{xy}E_y}{1 - \nu_{xy}\nu_{yx}} & \frac{E_y}{1 - \nu_{xy}\nu_{yx}} & 0 \\ 0 & 0 & G_{xy} \end{bmatrix} \begin{Bmatrix} \varepsilon_{x_0} \\ \varepsilon_{y_0} \\ \gamma_{xy_0} \end{Bmatrix}$$

$$\begin{aligned}
 & + \begin{bmatrix} \frac{zE_x}{1-g_{xy}g_{yx}} & \frac{z g_{yx} E_x}{1-g_{xy}g_{yx}} & 0 \\ \frac{z g_{xy} E_y}{1-g_{xy}g_{yx}} & \frac{zE_y}{1-g_{xy}g_{yx}} & 0 \\ 0 & 0 & G_{xy} \end{bmatrix} \begin{Bmatrix} -\frac{\partial w}{\partial x^2} \\ -\frac{\partial w}{\partial y^2} \\ -2\frac{\partial w}{\partial x \partial y} \end{Bmatrix} \quad (6) \\
 & - \frac{1}{1-g_{xy}g_{yx}} \begin{Bmatrix} E_x(\alpha_x(z) + g_{yx}\alpha_y(z)) \\ E_y(g_{xy}\alpha_x(z) + \alpha_y(z)) \\ 0 \end{Bmatrix} \Delta T \\
 & \frac{E_x}{g_{xy}} = \frac{E_y}{g_{yx}}
 \end{aligned}$$

### III. GOVERNING EQUATIONS

The governing equilibrium equation and compatibility equation for small deformations are considered here in (7) and (8), respectively [18]:

$$\frac{\partial^2 M_x}{\partial x^2} + 2\frac{\partial^2 M_{xy}}{\partial x \partial y} + \frac{\partial^2 M_y}{\partial y^2} = -q_z(x, y) \quad (7)$$

$$\frac{\partial^2 \varepsilon_x}{\partial y^2} + \frac{\partial^2 \varepsilon_y}{\partial x^2} = \frac{\partial^2 \gamma_{xy}}{\partial x \partial y} \quad (\gamma_{xy} = \gamma_{yz} = \varepsilon_z = 0) \quad (8)$$

$(N_x, N_y, N_{xy}), (M_x, M_y, M_{xy})$  are stress resultants and stress couples that may be obtained as follows:

$$\begin{aligned}
 & [(N_x, N_y, N_{xy}), (M_x, M_y, M_{xy})] = \\
 & \int_{-h/2}^{h/2} (1, z) (\sigma_x, \sigma_y, \tau_{xy}) dz
 \end{aligned} \quad (9)$$

$$(V_x, V_y) = \int_{-h/2}^{h/2} (\tau_{xz}, \tau_{yz}) dz \quad (10)$$

By substituting (9) and (10) into (6), stress resultants and stress couples are obtained:

$$\begin{Bmatrix} N_x \\ N_y \\ N_{xy} \end{Bmatrix} = \begin{bmatrix} A_{11} & A_{12} & 0 \\ A_{12} & A_{22} & 0 \\ 0 & 0 & A_{66} \end{bmatrix} \begin{Bmatrix} \varepsilon_{x_0} \\ \varepsilon_{y_0} \\ \gamma_{xy_0} \end{Bmatrix} \quad (11)$$

$$+ \begin{bmatrix} B_{11} & B_{12} & 0 \\ B_{12} & B_{22} & 0 \\ 0 & 0 & B_{66} \end{bmatrix} \begin{Bmatrix} -\frac{\partial^2 w}{\partial x^2} \\ -\frac{\partial^2 w}{\partial y^2} \\ -2\frac{\partial^2 w}{\partial x \partial y} \end{Bmatrix} \begin{Bmatrix} N_x^* \\ N_y^* \\ 0 \end{Bmatrix}$$

$$\begin{Bmatrix} M_x \\ M_y \\ M_{xy} \end{Bmatrix} = \begin{bmatrix} B_{11} & B_{12} & 0 \\ B_{12} & B_{22} & 0 \\ 0 & 0 & B_{66} \end{bmatrix} \begin{Bmatrix} \varepsilon_{x_0} \\ \varepsilon_{y_0} \\ \gamma_{xy_0} \end{Bmatrix} \quad (12)$$

$$+ \begin{bmatrix} C_{11} & C_{12} & 0 \\ C_{12} & C_{22} & 0 \\ 0 & 0 & C_{66} \end{bmatrix} \begin{Bmatrix} -\frac{\partial^2 w}{\partial x^2} \\ -\frac{\partial^2 w}{\partial y^2} \\ -2\frac{\partial^2 w}{\partial x \partial y} \end{Bmatrix} \begin{Bmatrix} M_x^* \\ M_y^* \\ 0 \end{Bmatrix}$$

$$(A_{11}, B_{11}, C_{11}) = \int_{-h/2}^{h/2} (1, z, z^2) \frac{E_x(z)}{1-g_{xy}g_{yx}} dz$$

$$(A_{12}, B_{12}, C_{12}) = \int_{-h/2}^{h/2} (1, z, z^2) \frac{g_{yx} E_x(z)}{1-g_{xy}g_{yx}} dz$$

$$(A_{22}, B_{22}, C_{22}) = \int_{-h/2}^{h/2} (1, z, z^2) \frac{E_y(z)}{1-g_{xy}g_{yx}} dz$$

$$(A_{66}, B_{66}, C_{66}) = \int_{-h/2}^{h/2} (1, z, z^2) G_{xy}(z) dz$$

$$(N_x^*, M_x^*) =$$

$$\frac{1}{1-g_{xy}g_{yx}} \int_{-h/2}^{h/2} E_x(z) (\alpha_x(z) + g_{yx}\alpha_y(z)) (1, z) \Delta T dz$$

$$(N_y^*, M_y^*) =$$

$$\frac{1}{1-g_{xy}g_{yx}} \int_{-h/2}^{h/2} E_y(z) (g_{xy}\alpha_x(z) + \alpha_y(z)) (1, z) \Delta T dz$$

$$\beta = \frac{N_y^*}{N_x^*} = \frac{M_y^*}{M_x^*}, \mu = \frac{\alpha_y}{\alpha_x}, (N^*, M^*) = (N_x^*, M_x^*)$$

We introduce Airy stress function  $\phi(x, y)$ , which is defined by:

$$N_x = \frac{\partial^2 \phi}{\partial y^2}, N_y = \frac{\partial^2 \phi}{\partial x^2}, N_{xy} = -\frac{\partial^2 \phi}{\partial x \partial y} \quad (13)$$

Substituting (13) for (11) and (12), we can derive the strain components in the middle surface and stress couples as follows:

$$\begin{Bmatrix} \varepsilon_{x_0} \\ \varepsilon_{y_0} \\ \varepsilon_{xy_0} \end{Bmatrix} = \begin{bmatrix} D_{11} & D_{12} & 0 \\ D_{12} & D_{22} & 0 \\ 0 & 0 & D_{66} \end{bmatrix} \begin{Bmatrix} \frac{\partial^2 \phi}{\partial y^2} \\ \frac{\partial^2 \phi}{\partial x^2} \\ \frac{\partial^2 \phi}{\partial x \partial y} \end{Bmatrix}$$

$$+ \begin{bmatrix} F_{11} & F_{12} & 0 \\ F_{12} & F_{22} & 0 \\ 0 & 0 & F_{66} \end{bmatrix} \begin{Bmatrix} -\frac{\partial^2 w}{\partial x^2} \\ -\frac{\partial^2 w}{\partial y^2} \\ -2\frac{\partial^2 w}{\partial x \partial y} \end{Bmatrix} + \begin{Bmatrix} H_{11} \\ H_{21} \\ 0 \end{Bmatrix} N^* \quad (14-1)$$

$$\begin{Bmatrix} M_x \\ M_y \\ M_{xy} \end{Bmatrix} = \begin{bmatrix} -F_{11} & -F_{12} & 0 \\ -F_{12} & -F_{22} & 0 \\ 0 & 0 & -F_{66} \end{bmatrix} \begin{Bmatrix} \frac{\partial^2 \phi}{\partial y^2} \\ \frac{\partial^2 \phi}{\partial x^2} \\ \frac{\partial^2 \phi}{\partial x \partial y} \end{Bmatrix} \quad (15)$$

$$+ \begin{bmatrix} I_{11} & I_{12} & 0 \\ I_{12} & I_{22} & 0 \\ 0 & 0 & I_{66} \end{bmatrix} \begin{Bmatrix} -\frac{\partial^2 w}{\partial x^2} \\ -\frac{\partial^2 w}{\partial y^2} \\ -2\frac{\partial^2 w}{\partial x \partial y} \end{Bmatrix} + \begin{Bmatrix} J_{11} \\ J_{21} \\ 0 \end{Bmatrix} M^*$$

$$\theta = A_{11}A_{22} - A_{12}^2$$

$$D_{11} = A_{22} / \theta$$

$$D_{12} = -A_{12} / \theta$$

$$F_{11} = (A_{12}B_{12} - B_{11}A_{22}) / \theta$$

$$F_{12} = (A_{12}B_{22} - A_{22}B_{12}) / \theta$$

$$F_{21} = (A_{12}B_{11} - A_{11}B_{12}) / \theta$$

$$\begin{aligned}
 D_{22} &= A_{11} / \theta & F_{22} &= (A_{12}B_{12} - A_{11}B_{22}) / \theta \\
 D_{66} &= -1 / A_{66} & F_{66} &= -B_{66} / A_{66} \\
 H_{11} &= (A_{22} - \beta A_{12}) / \theta & I_{11} &= B_{11}F_{11} + B_{12}F_{21} + C_{11} \\
 H_{21} &= (\beta A_{11} - A_{12}) / \theta & I_{12} &= B_{11}F_{12} + B_{12}F_{22} + C_{12} \\
 J_{11} &= \eta(\beta F_{21} + F_{11}) + 1 & I_{21} &= B_{12}F_{11} + B_{22}F_{21} + C_{12} \\
 J_{21} &= \eta(\beta F_{22} + F_{12}) + \beta & I_{22} &= B_{12}F_{12} + B_{22}F_{22} + C_{22} \\
 N^* &= \eta M^* & I_{66} &= C_{66} - (B_{66}^2 / A_{66})
 \end{aligned}$$

Using (7) with (15) and (8) with (14), the governing equation is rewritten in terms of Airy stress function and deflection as follows:

$$\begin{aligned}
 F_{21} \frac{\partial^4 \phi}{\partial x^4} + (F_{11} + F_{22} - 2F_{66}) \frac{\partial^4 \phi}{\partial x^2 \partial y^2} + F_{12} \frac{\partial^4 \phi}{\partial y^4} \\
 + I_{11} \frac{\partial^4 w}{\partial x^4} + (2I_{12} + 4I_{66}) \frac{\partial^4 w}{\partial x^2 \partial y^2} + I_{22} \frac{\partial^4 w}{\partial y^4} \\
 + J_{11} \frac{\partial^2 M^*}{\partial x^2} + J_{21} \frac{\partial^2 M^*}{\partial y^2} = q_z(x, y)
 \end{aligned} \quad (16)$$

$$\begin{aligned}
 D_{11} \frac{\partial^4 \phi}{\partial y^4} + D_{22} \frac{\partial^4 \phi}{\partial x^4} + (2D_{12} - D_{66}) \frac{\partial^4 \phi}{\partial x^2 \partial y^2} \\
 - F_{21} \frac{\partial^4 w}{\partial x^4} - F_{12} \frac{\partial^4 w}{\partial y^4} + (2F_{66} - F_{11} - F_{22}) \frac{\partial^4 w}{\partial x^2 \partial y^2} \\
 + \eta H_{21} \frac{\partial^2 M^*}{\partial x^2} + \eta H_{11} \frac{\partial^2 M^*}{\partial y^2} = 0
 \end{aligned} \quad (17)$$

#### Exact Solution

Assuming being four edges of plate in simply supported conditions, the functions of deflection, Airy stress function, thermal moment and transverse loading are expressed as double Fourier series as follows:

$$\begin{aligned}
 w(x, y) &= \sum_m \sum_n w_{mn} \sin \frac{m\pi x}{a} \sin \frac{n\pi y}{b} \\
 \phi(x, y) &= \sum_m \sum_n \phi_{mn} \sin \frac{m\pi x}{a} \sin \frac{n\pi y}{b} \\
 M^*(x, y) &= \sum_m \sum_n T_{mn} \sin \frac{m\pi x}{a} \sin \frac{n\pi y}{b} \\
 q_z(x, y) &= \sum_m \sum_n q_{mn} \sin \frac{m\pi x}{a} \sin \frac{n\pi y}{b}
 \end{aligned} \quad (18)$$

where,

$$T_{mn} = \begin{cases} 16M^* & m, n = 1, 3, 5, \dots \\ \pi^2 mn & m, n = 2, 4, 6, \dots \\ 0 & \end{cases} \quad (19)$$

$$q_{mn} = \begin{cases} 16q_0 & m, n = 1, 3, 5, \dots \\ \pi^2 mn & m, n = 2, 4, 6, \dots \\ 0 & \end{cases} \quad (20)$$

Upon substituting (20) for (17-18),  $w_{mn}, \phi_{mn}$  is obtained as follows:

$$\begin{aligned}
 w_{mn} &= \frac{1}{K^2 + RL} [Lq_{mn} + (SL - KQ)T_{mn}] \\
 \phi_{mn} &= \frac{1}{K^2 + RL} [Kq_{mn} + (SK + RQ)T_{mn}]
 \end{aligned} \quad (21)$$

Where,

$$\begin{aligned}
 L &= D_{11} \left(\frac{n\pi}{b}\right)^4 + D_{22} \left(\frac{m\pi}{a}\right)^4 + (2D_{12} - D_{66}) \left(\frac{m\pi}{a}\right)^2 \left(\frac{n\pi}{b}\right)^2 \\
 K &= F_{21} \left(\frac{m\pi}{a}\right)^4 + (F_{11} + F_{22} - 2F_{66}) \left(\frac{m\pi}{a}\right)^2 \left(\frac{n\pi}{b}\right)^2 + F_{12} \left(\frac{n\pi}{b}\right)^4 \\
 R &= I_{11} \left(\frac{m\pi}{a}\right)^4 + (2I_{12} + 4I_{66}) \left(\frac{m\pi}{a}\right)^2 \left(\frac{n\pi}{b}\right)^2 + I_{22} \left(\frac{n\pi}{b}\right)^4 \\
 Q &= \eta \left[ H_{21} \left(\frac{m\pi}{a}\right)^2 + H_{11} \left(\frac{n\pi}{b}\right)^2 \right] \\
 S &= J_{11} \left(\frac{m\pi}{a}\right)^2 + J_{21} \left(\frac{n\pi}{b}\right)^2
 \end{aligned}$$

Therefore, by substituting (18) for (14) and (6), the strain components and stress field for any arbitrary point across thickness are determined. (See appendix)

#### IV. Numerical Results

##### Convergence of Results

In this section, using the datum in [4], the reliability and exactness of results are investigated. The thermoelastic response of isotropic FG square plate having  $p = 2, a = 100\text{cm}, b = 100\text{cm}, h = 2\text{cm}, \vartheta = 0.3, q_0 = 1\text{kg/cm}^2, E_1 = 2.1 \times 10^6\text{kg/cm}^2$  is studied.

As table 1 reveals, increasing m, n more than 20 has no magnificent change to determine the stress and deflection; hence m and n are taken 20 to perform the numerical results.

Table 1. Convergence of numerical result

$m, n$	$w(\text{cm})$	$\sigma_x = (\text{kg/cm}^2)$
20	0.37369615898	-105.868598
50	0.37369652377	-105.892742
100	0.37369651982	-105.891072
200	0.37369651994	-105.891234
300	0.37369651994	-105.891250
400	0.37369651994	-105.891254

##### Validation

In this section, in order to validate the numerical results, comparison is performed with [4].

Table 2 and 3 show that good agreement is observed between present study and the previous studies.

Table 2. The comparison of numerical results

$E_1 / E_2$	Present			Chi and Chung[4]		
	$w/h$	$\varepsilon_x$	$\sigma_x / q_0$	$w/h$	$\varepsilon_x$	$\sigma_x / q_0$
1	0.1320263	0.0002394	718.14199	0.1320263	0.0002394	718.14199
1.5	0.1618025	0.0002689	806.76377	0.1618025	0.0002689	806.76377
2	0.1868481	0.0002917	875.18041	0.1868481	0.0002917	875.18041
4	0.2599903	0.0003535	1060.6405	0.2599903	0.0003535	1060.6405
10	0.368543	0.0004404	1321.2446	0.368543	0.0004404	1321.2446
30	0.4695579	0.0005195	1558.5538	0.4695579	0.0005195	1558.5538

Table 3. The comparison of numerical results for non-dimensional displacement

Theory	$\bar{w}$				$\bar{\sigma}_x$
	$a/b=2$	$a/b=3$	$a/b=4$	$a/b=5$	
Present work	0.390824	0.1870834	0.106762	0.0684987	-1.917719
Houari et al. [16]	0.270902	0.141810	0.088642	0.062334	-1.963621
Zenkour & Alghamdi [14]	0.273492	0.136798	0.080512	0.052678	-1.764689

*The influence of orthotropic ratio*

As observed in Fig. 3 by increasing Young modulus ratio (Plate 1 to Plate 4), the distribution of stress across the thickness possesses more nonlinear form. In addition, the location of neutral surface moves toward the surface with stronger properties. In Fig. 4, the maximum  $w/h$  allocated for plate 1 equals 0.239 and for plate 2, plate 3 and plate 4 equal 0.234, 0.2 and 0.167, respectively. As shown in Fig. 5, the variation of stress in plate 4 is pronouncedly higher than the other cases, due to exposing to thermal gradient.

Table 4. The material properties of Plate 1

Material property lower surface	
$E_{x1} = 1.5 \times E_{x2}$	$\alpha_{x1} = 1.5 \times \alpha_{x2}$
$E_{y1} = 1.5 \times E_{y2}$	$\alpha_{y1} = 1.5 \times \alpha_{y2}$
$G_{xy1} = 1.5 \times G_{xy2}$	
Material properties of upper surface for the 100% alumina surface[19]	
$E_{x2} = 1.1861 \times 10^6 \text{ kg/cm}^2$	$\alpha_{x2} = 7.5 \times 10^{-6} (\text{°C})^{-1}$
$E_{y2} = 0.9218 \times 10^6 \text{ kg/cm}^2$	$\alpha_{y2} = 8 \times 10^{-6} (\text{°C})^{-1}$
$G_{xy2} = 0.3895 \times 10^6 \text{ kg/cm}^2$	

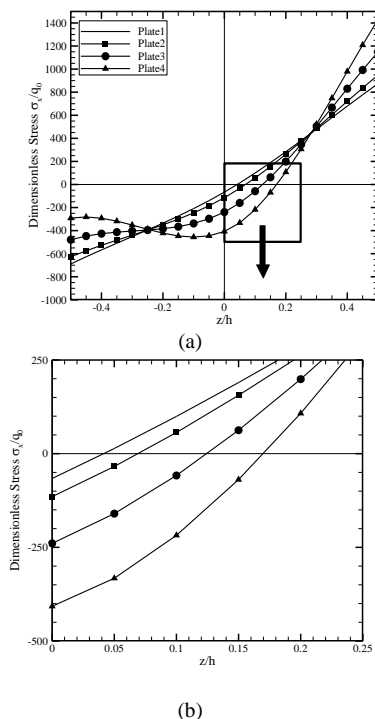


Fig. 3. Variation of non-dimensional stress across the thickness ( $T = 0^\circ\text{C}, q_0 = 1 \text{ kg/cm}^2$ )

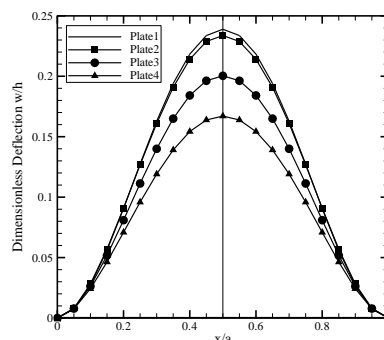


Fig. 4. Distribution of deflection along the x-direction with thermal gradient

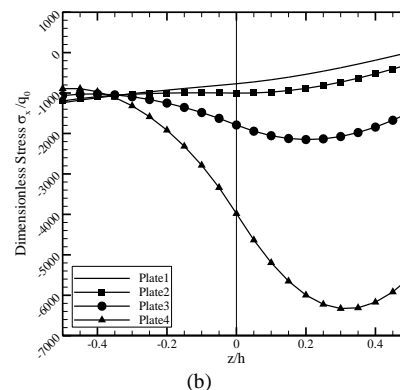
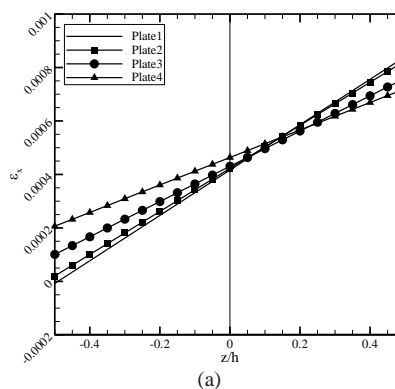


Fig. 5. Variation of a) axial strain b) axial non-dimensional stress across the thickness ( $T = 100^\circ\text{C}, q_0 = 1 \text{ kg/cm}^2$ )

*Effect of Thermal Gradient*

In order to examine the influence of thermal gradient on bending subjected on mechanical loading, a FG plate with two constituent materials Nickel as metal and Alumina ( $\text{Al}_2\text{O}_3$ ) as ceramics is considered. It is assumed that Nickel and Alumina are isotropic and have orthotropic characteristics, respectively. For simplicity, Poisson ratios are chosen as constant values,  $\nu_{xy} = 0.3, \nu_{yx} = 0.26$ . The data used in the numerical results as sketched in Figs 7-9, are taken as table 5.

Table 5. Material properties of FG plate

Material property (1) data for the 100% nickel surface	
$E_{x1} = 2.0795 \times 10^6 \text{ kg / cm}^2$	$\alpha_{x1} = 13.3 \times 10^{-6} (\text{°C})^{-1}$
$E_{y1} = 2.0795 \times 10^6 \text{ kg / cm}^2$	$\alpha_{y1} = 13.3 \times 10^{-6} (\text{°C})^{-1}$
$G_{yy1} = 0.7941 \times 10^6 \text{ kg / cm}^2$	
Material property (2) data for the 100% alumina surface	
$E_{x2} = 1.1861 \times 10^6 \text{ kg / cm}^2$	$\alpha_{x2} = 7.5 \times 10^{-6} (\text{°C})^{-1}$
$E_{y2} = 0.9218 \times 10^6 \text{ kg / cm}^2$	$\alpha_{y2} = 8 \times 10^{-6} (\text{°C})^{-1}$
$G_{xy2} = 0.3895 \times 10^6 \text{ kg / cm}^2$	

As depicted in Fig. 6, the increasing in aspect ratio causes the decrease in non-dimensional central deflection. As observed, the deflection due to thermomechanical loading is the superposition of deflections of thermal gradient and mechanical loading, separately.

In Fig. 7, the distribution of  $\sigma_x$ ,  $\sigma_y$  across the thickness is sketched with respect to variation of aspect ratio. As observed, with increasing aspect ratio higher than 5, the variation of stress does not change appreciably. This trend is observed in Fig. 8 for the variation of  $\varepsilon_x$ ,  $\varepsilon_y$  with respect to the foregoing ratio.

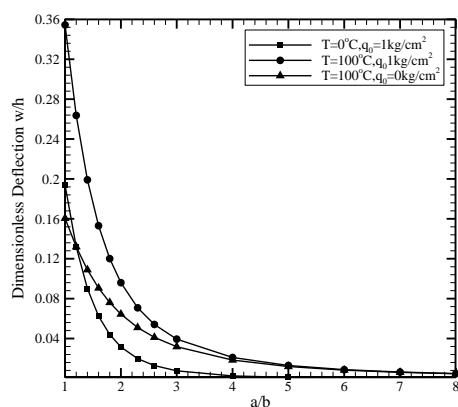


Fig. 6. Maximum deflection with respect to aspect ratio at different temperature gradients

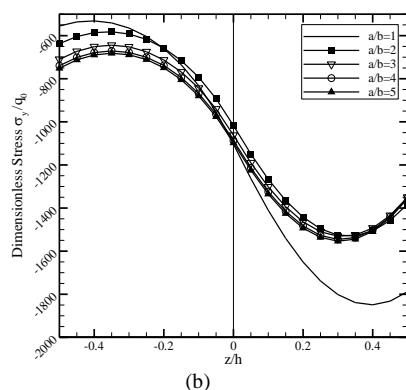
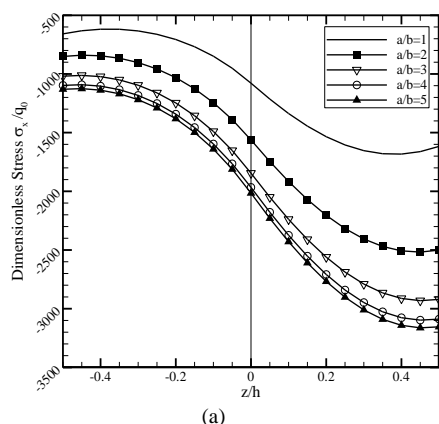


Fig. 7. Influence of aspect ratio on distribution of non-dimensional stress at  $T=100^\circ\text{C}$ .

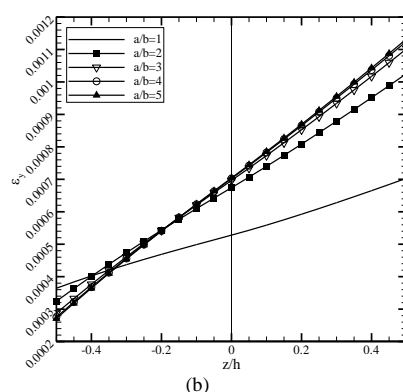
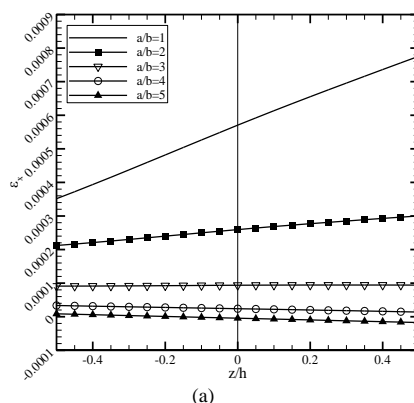


Fig. 8. Influence of aspect ratio on distribution of plane strain at  $T=100^\circ\text{C}$ .

## V. CONCLUSION

In this paper, the thermoelastic response of a thin orthotropic FG plate when subjected to thermomechanical loading is discussed. The influence of the variation of aspect ratio and mechanical properties on deflection and stresses is considered. Some of the novelties of the present study are:

With increasing Young modulus ratio of two faces of plate, the location of the neutral plane is changed and moves toward the surface having greater properties. As observed by adding thermal gradient to the plate, the neutral plane is eliminated and the sign of stresses is changed to negative (compression stress).

In case of applying more intensity of mechanical loading, the values of  $\sigma_x$ ,  $\sigma_y$  are increased while the values of  $\varepsilon_x$ ,  $\varepsilon_y$  are decreased; whereas by adding thermal gradient, this

trend becomes converse.

It is noted that in orthotropic FG plate, when raising the working temperature of plate, by increasing aspect ratio, the intensity of thermal stress  $\sigma_x$  and thermal strain  $\varepsilon_x$  are

increased while  $\sigma_y$  and  $\varepsilon_y$  are diminished. For aspect ratio greater than 5, this trend remains almost constant.

#### Appendix

$$\varepsilon_x = \sum_m \sum_n \frac{q_{mn}}{K^2 + RL} \left\{ [(F_{11} + z)L - KD_{12} \left( \frac{m\pi}{a} \right)^2 - KD_{11} \left( \frac{n\pi}{b} \right)^2] \sin \frac{m\pi x}{a} \sin \frac{n\pi y}{b} \right. \quad (A-1)$$

$$\left. + \sum_m \sum_n \frac{T_{mn}}{K^2 + RL} \left\{ [(F_{11} + z)(SL - KQ)D_{12} \left( \frac{m\pi}{a} \right)^2 - (SK + RQ)D_{11} \left( \frac{n\pi}{b} \right)^2] \sin \frac{m\pi x}{a} \sin \frac{n\pi y}{b} \right. \right.$$

$$\left. + \eta(K^2 + RL)H_{11} \right\} \varepsilon_y = \sum_m \sum_n \frac{q_{mn}}{K^2 + RL} \left\{ -KD_{22} \left( \frac{m\pi}{a} \right)^2 + [(F_{22} + z)L - KD_{12} \left( \frac{n\pi}{b} \right)^2] \sin \frac{m\pi x}{a} \sin \frac{n\pi y}{b} \right. \quad (A-2)$$

$$\left. + \sum_m \sum_n \frac{T_{mn}}{K^2 + RL} \left\{ -(SK + RQ)D_{22} \left( \frac{m\pi}{a} \right)^2 \right. \right.$$

$$\left. + [(F_{22} + z)(SL - KQ) - (SK + RQ)D_{12} \left( \frac{n\pi}{b} \right)^2 + \eta(K^2 + RL)H_{21}] \right\} \sin \frac{m\pi x}{a} \sin \frac{n\pi y}{b} \quad (A-3)$$

$$\gamma_{xy} = \sum_m \sum_n \frac{q_{mn}}{K^2 + RL} [KD_{66} - 2L(F_{66} + z)] \left( \frac{m\pi}{a} \right) \left( \frac{n\pi}{b} \right) \cos \frac{m\pi x}{a} \cos \frac{n\pi y}{b}$$

$$+ \sum_m \sum_n \frac{T_{mn}}{K^2 + RL} [(SK + RQ)D_{66} - 2(SL - KQ)(F_{66} + z)] \left( \frac{m\pi}{a} \right) \left( \frac{n\pi}{b} \right) \cos \frac{m\pi x}{a} \cos \frac{n\pi y}{b}$$

#### REFERENCES

- [1] Niino, A., Maeda, S., "Recent development status of functionally graded materials." ISIJ International 30, 1990, 699-703.
- [2] Hirano, T., Yamada, T., "Multi-paradigm expert system architecture based upon the inverse design concept." International Workshop on Artificial Intelligence for Industrial Applications, Hitachi, Japan, 1988, 25-27.
- [3] Chi, S.H., and Chung, Y.L., "Cracking in sigmoid functionally graded coating". Journal of Mechanics 18, 2002, 41-53.
- [4] Chi S.H., and Chung Y.L., "Mechanical Behavior of Functionally Graded Material Plates Under Transverse Load", I: Analysis, Int. J. Solids Struct., 43, 13, 2006, 3657-3674.
- [5] Chi S.H., and Chung Y.L., "Mechanical Behavior of Functionally Graded Material Plates under Transverse Load", II: Numerical results. Int.J. Solids Struct. 43, 13, 2006, 3675-3691.
- [6] Bao G, Jiang W, Roberts JC. "Analytic and finite element solutions for bending and buckling of orthotropic rectangular plates." Int. J. Solids Struct. 1997; 34(14):1797-822.
- [7] Bhaskar K, and Kaushik B. "Simple and exact series solutions for flexure of orthotropic rectangular plates with any combination of clamped and simply supported edges. Compos." Struct. 2004;63(1):63-8.
- [8] Khov H, Li WL, Gibson RF. "An accurate solution method for the static and dynamic deflections of orthotropic plates with general boundary conditions." Compos. Struct. 2009;90(4):474-81.
- [9] Li R, Zhong Y, Tian B, Liu Y. "On the finite integral transform method for exact bending solutions of fully clamped orthotropic rectangular thin plates." Appl. Math. Lett. 2009;22(12):1821-7.
- [10] Morimoto T., and Tanigawa Y., "Linear Buckling Analysis of Orthotropic Inhomogeneous Rectangular Plates under Uniform In-Plane Compression", Acta Mechanica, 187, 2006, 219-229.
- [11] Ghannadpour S.A.M., and Alinia M.M., "Large Deflection Behavior of Functionally Graded Plates under Pressure Loads", Composite Structures, 75, 2006, 67-71.
- [12] Alinia M.M., and Ghannadpour S.A.M., "Nonlinear Analysis of Pressure Loaded FGM Plates", Composite Structures, 88, 2009, 354-359.
- [13] Chung Yen-Ling., and Chen Wei-Ting., "The Flexibility of Functionally Graded Material Plates Subjected to Uniform Loads", Journal of mechanics of materials and structures, vol.2, 1, 2007, 63-86.
- [14] Zenkour A.M., Alghamdi N.A., "Thermoelastic Bending Analysis of Functionally Graded Sandwich Plates", Journal of materials science, 43, 2008, 2574-2589.
- [15] Beom H.G, "Thermoelastic In-Plane Fields in a Linear Anisotropic Solid", International Journal of Engineering Science, 69, 2013, 49-60.
- [16] Houari MSA., and Tounsi A., and Bég OA, "Thermoelastic Bending Analysis of Functionally Graded Sandwich Plates Using a New Higher Order Shear and Normal Deformation Theory". Int J Mech Sci, 76, 2013, 102-111.
- [17] Serkan Dag, and Erhan Arman E., and Bora Yildirim, "Computation of Thermal Fracture Parameters for Orthotropic Functionally Graded Materials Using Jk-Integral", International journal of solids and structures, 47, 2010, 3480-3488.
- [18] Ugural A., "Stress in Plates and Shells", McGraw-Hill Book Company, 1981.
- [19] Serkan Dag, "Thermal Fracture Analysis of Orthotropic Functionally Graded Materials Using an Equivalent Domain Integral Approach", Engineering Fracture Mechanics, 73, 2006, 2802-2828.